Winter weather controls net influx of atmospheric CO2 on the north-west European shelf

Vassilis Kitidis, Jamie Shutler, Ian Ashton, Mark Warren, Ian Brown, Helen Findlay, Sue Hartman, Richard Sanders, Matthew P. Humphreys, Caroline Kivimäe, et al.

SCIENTIFIC REPORTS
nature research

OPEN

Winter weather controls net influx of atmospheric CO_2 on the north-west European shelf

Vassilis Kitidis[1*], Jamie D. Shutler[2], Ian Ashton[2], Mark Warren[1], Ian Brown[1], Helen Findlay[1], Sue E. Hartman[3], Richard Sanders[3], Matthew Humphreys[4,22], Caroline Kivimäe[3], Naomi Greenwood[5], Tom Hull[5], David Pearce[5], Triona McGrath[6], Brian M. Stewart[7], Pamela Walsham[8], Evin McGovern[9], Yann Bozec[10], Jean-Philippe Gac[10], Steven M. A. C. van Heuven[11], Mario Hoppema[12], Ute Schuster[2], Truls Johannessen[13], Abdirahman Omar[14], Siv K. Lauvset[14], Ingunn Skjelvan[14], Are Olsen[13], Tobias Steinhoff[15], Arne Körtzinger[15], Meike Becker[15,23], Nathalie Lefevre[16], Denis Diverrès[17], Thanos Gkritzalis[18], André Cattrijsse[18], Wilhelm Petersen[19], Yoana G. Voynova[19], Bertrand Chapron[20], Antoine Grouazel[20], Peter E. Land[1], Jonathan Sharples[21] & Philip D. Nightingale[1]

Shelf seas play an important role in the global carbon cycle, absorbing atmospheric carbon dioxide (CO_2) and exporting carbon (C) to the open ocean and sediments. The magnitude of these processes is poorly constrained, because observations are typically interpolated over multiple years. Here, we used 298500 observations of CO_2 fugacity (fCO_2) from a single year (2015), to estimate the net influx of atmospheric CO_2 as 26.2 ± 4.7 Tg C yr^{-1} over the open NW European shelf. CO_2 influx from the atmosphere was dominated by influx during winter as a consequence of high winds, despite a smaller, thermally-driven, air-sea fCO_2 gradient compared to the larger, biologically-driven summer gradient. In order to understand this climate regulation service, we constructed a carbon-budget supplemented by data from the literature, where the NW European shelf is treated as a box with carbon entering and leaving the box. This budget showed that net C-burial was a small sink of 1.3 ± 3.1 Tg C yr^{-1}, while CO_2 efflux from estuaries to the atmosphere, removed the majority of river C-inputs. In contrast, the input from the Baltic Sea likely contributes to net export via the continental shelf pump and advection (34.4 ± 6.0 Tg C yr^{-1}).

[1]Plymouth Marine Laboratory, Plymouth, UK. [2]University of Exeter, College of Life and Environmental Sciences, Exeter, UK. [3]National Oceanography Centre, Southampton, UK. [4]Ocean and Earth Science, University of Southampton, Southampton, UK. [5]Centre for Environment Fisheries and Aquaculture Science (Cefas), Lowestoft, UK. [6]National University of Ireland, Galway, Ireland. [7]Agri-Food and Biosciences Institute, Belfast, UK. [8]Marine Scotland Science (MSS), Aberdeen, UK. [9]The Marine Institute, Galway, Ireland. [10]Station Biologique de Roscoff, UMR CNRS - UPMC 7144 - Equipe Chimie Marine, Roscoff, France. [11]University of Groningen, Faculty of Science and Engineering, Groningen, Netherlands. [12]Alfred Wegener Institute, Helmholtz Centre for Polar and Marine Research, Bremerhaven, Germany. [13]Geophysical Institute, University of Bergen and Bjerknes Center for Climate Research, Bergen, Norway. [14]NORCE Norwegian Research Centre, Bjerknes Center for Climate Research, Bergen, Norway. [15]GEOMAR Helmholtz Centre for Ocean Research Kiel, Kiel, Germany. [16]Sorbonne Universités (UPMC, Univ Paris 06)-IRD-CNRS-MNHN, LOCEAN, Paris, France. [17]Institut de Recherche pour le Développement (IRD), centre de Bretagne, Plouzané, France. [18]VLIZ Flanders Marine Institute, Ostend, Belgium. [19]Helmholtz Zentrum Geesthacht, Centre for Materials and Coastal Research, Geesthacht, Germany. [20]Institut Francais Recherche Pour LExploitation de la Mer, Pointe du Diable, 29280, Plouzané, France. [21]University of Liverpool, School of Environmental Sciences, Liverpool, UK. [22]Present address: School of Environmental Sciences, University of East Anglia, Norwich, UK. [23]Present address: Geophysical Institute, University of Bergen and Bjerknes Center for Climate Research, Bergen, Norway. *email: vak@pml.ac.uk

Temperate continental shelf seas (<200 m depth) occupy ~7% of the ocean surface area, yet contribute disproportionately to net marine drawdown of atmospheric carbon dioxide (CO_2), accounting for 10–20% of the global total net uptake[1–3]. Century-scale storage of this CO_2 in sediments and seawater results in a substantial climate regulation service, but has also caused ocean acidification (OA), a reduction in pH which is projected to continue as atmospheric CO_2 increases[4]. Net atmospheric CO_2 drawdown in temperate shelf seas is mediated by physical processes (dissolution of CO_2) and nutrient-limited net community production (NCP: photosynthesis minus mineralization). Predictions of the future drawdown of atmospheric CO_2 are highly contradictory. On the one hand, increasing CO_2 in the atmosphere is expected to enhance the air to sea flux of CO_2, simply by driving the respective concentration gradient. However, the inverse dependence of CO_2 solubility on temperature[5] may limit this flux as sea surface temperature (SST) increases. In contrast with observations showing a 35-year increase in shelf sea CO_2 drawdown over the NW European shelf[6], models predict a future decrease as a result of reduced nutrient supply and net biological CO_2 uptake[7,8]. Other models suggest that saturation of the 'continental shelf pump' [CSP; the seasonal C export into intermediate waters of the open ocean[9]] may limit further drawdown from the atmosphere[10].

Net air to sea CO_2 flux may be calculated from ship-board observations of CO_2 fugacity (fCO_2; the partial pressure of CO_2 corrected for its non-ideal-gas behaviour). Here, we evaluate the air to sea CO_2 flux for the NW European shelf based on the most geographically-extensive, single-year, fCO_2 dataset to date. Compared to previous evaluations (based on regional data extrapolation and combination of multiannual observations), this unique dataset provides a detailed snapshot of the air to sea CO_2 flux.

The NW European shelf is hydrologically linked to the surrounding land-mass where temperature, precipitation and river-runoff are projected to increase over the next 50 years[11,12]. Policies regulating the application of fertilisers and wastewater treatment[13–16] have reduced the nutrient loading on land and river-borne inputs to the shelf and may thereby alter the biological component of the air to sea CO_2 flux. Similarly, changes in riverine dissolved organic C (DOC) inputs have the potential to modify shelf C-budgets as DOC is mineralized in shelf seas and returned to the atmosphere as CO_2[17]. The recent trend of decreasing DOC input from major UK rivers (since 2000) has been attributed to implementation of the urban sewage treatment directive[18]. This followed an earlier trend of increasing DOC flux from rivers across the northern hemisphere which was attributed to soil recovery from acid rain after implementation of sulphur emission policies[17]. A comprehensive, observation-based analysis of the relative magnitude of C-fluxes on the NW European shelf which would allow us to constrain the potential impact of these feedbacks is currently missing. In order to address this, we have constructed a balanced budget based on observed C-fluxes on the NW European shelf (including air to sea CO_2 flux, riverine and Baltic Sea inputs, inorganic C accumulation, C-burial and export via the CSP and advection). This enables an investigation of the factors controlling the air to sea flux, in turn providing guidance on the impact of land management practices.

Results

Air to sea flux in 2015. Monthly average fluxes showed considerable spatial and seasonal variability over 2015 (Fig. 1), reflecting changes in phytoplankton abundance, CO_2 solubility and wind speed which generates turbulence at the air-sea interface promoting flux (Fig. 1 and Supplementary Figs. 1–3). The interplay between physical and biological processes can be used to explain the seasonal distribution of air to sea CO_2 flux. For example, NCP contributes to the uptake of CO_2. Variability in Chlorophyll-a[19] was used as a proxy for NCP (Supplementary Fig. 1). Chlorophyll-a is weakly correlated with phytoplankton biomass so that monthly changes in the former are at least qualitatively related to NCP and by extension biological CO_2 uptake or release[20]. A monthly increase in Chlorophyll-a thereby indicates net primary production (positive NCP), while a decrease suggests net respiration (negative NCP). In the Celtic Sea and central North Sea, high influx of CO_2 from the atmosphere was found in spring/summer coincident with the highest surface Chlorophyll-a concentrations (correlation at −7.5 °E, 50 °N and 6 °E, 55 °N; Apr-Jul; $R^2 = 0.47$; $p < 0.05$, $n = 8$). It is important to note that the distributions of air-sea CO_2 flux and Chlorophyll-a are not perfectly anti-correlated, even during this net phytoplankton growth period, likely due to subsurface primary production in summer[21], hysteresis in $fCO_{2\,sea}$ re-equilibration with $fCO_{2\,air}$[22] and other factors. The apparently high levels of Chlorophyll-a found in winter (Dec. to Feb.), particularly in shallow coastal areas, are likely due to coloured organic matter and sediment reflectance rather than Chlorophyll-a [i.e., Case II waters[23]], (Supplementary Fig. 1). The solubility of CO_2 (α_{sea} in Eq. 1; a function of seawater temperature and salinity; Supplementary Fig. 2) contributes to the potential in-water-CO_2-concentration ($fCO_{2\,sea}$ in Eq. 1) and thus the ΔfCO_2 ($fCO_{2\,sea}$ - $fCO_{2\,air}$). Thereby, lower α_{sea} in the southern North Sea in summer as well as remineralization of river-borne organic matter[24,25] likely contribute to the efflux of CO_2 to the atmosphere in this region. Finally, wind speed (U10; Supplementary Fig. 3), determines the gas transfer coefficient (k in Eq. 1). Wind speed was 49% higher in winter to early spring (Dec-Mar) compared to summer (Jun-Aug), resulting in 149% greater k values in winter and high drawdown of atmospheric CO_2.

The net-integrated air to sea flux of CO_2 for 2015 within the region defined by the 200 m isobath was 26.2 ± 4.7 Tg y^{-1} (Fig. 2c). Including the Norwegian trench, the net influx of CO_2 from the atmosphere was 26.7 ± 4.8 Tg y^{-1}. $fCO_{2\,sea}$ and air to sea flux were further separated into thermal (e.g. due to cooling-enhanced solubility) and biological + mixing components following Eqs. 2 and 3. In 2015, the mean biological + mixing component ($fCO_{2\,bio}$) closely matched the seasonal pattern of $fCO_{2\,sea}$ over the domain with lower $fCO_{2\,sea}$ in spring/summer (Fig. 2a). In contrast the air to sea CO_2 flux and its thermal component, were highest in winter, (Fig. 2b,c). A concomitant increase in the gas transfer velocity was evident in winter (Fig. 2b). The annual mean thermal to biological + mixing components ratio was thereby 2.1 ± 1.7 (where the uncertainty given is one standard deviation). The highest values for this ratio, indicating thermal-flux-component dominance, were observed in the western Hebridean Shelf, English Channel and northern Celtic Sea (Fig. 2d). This was largely due to low

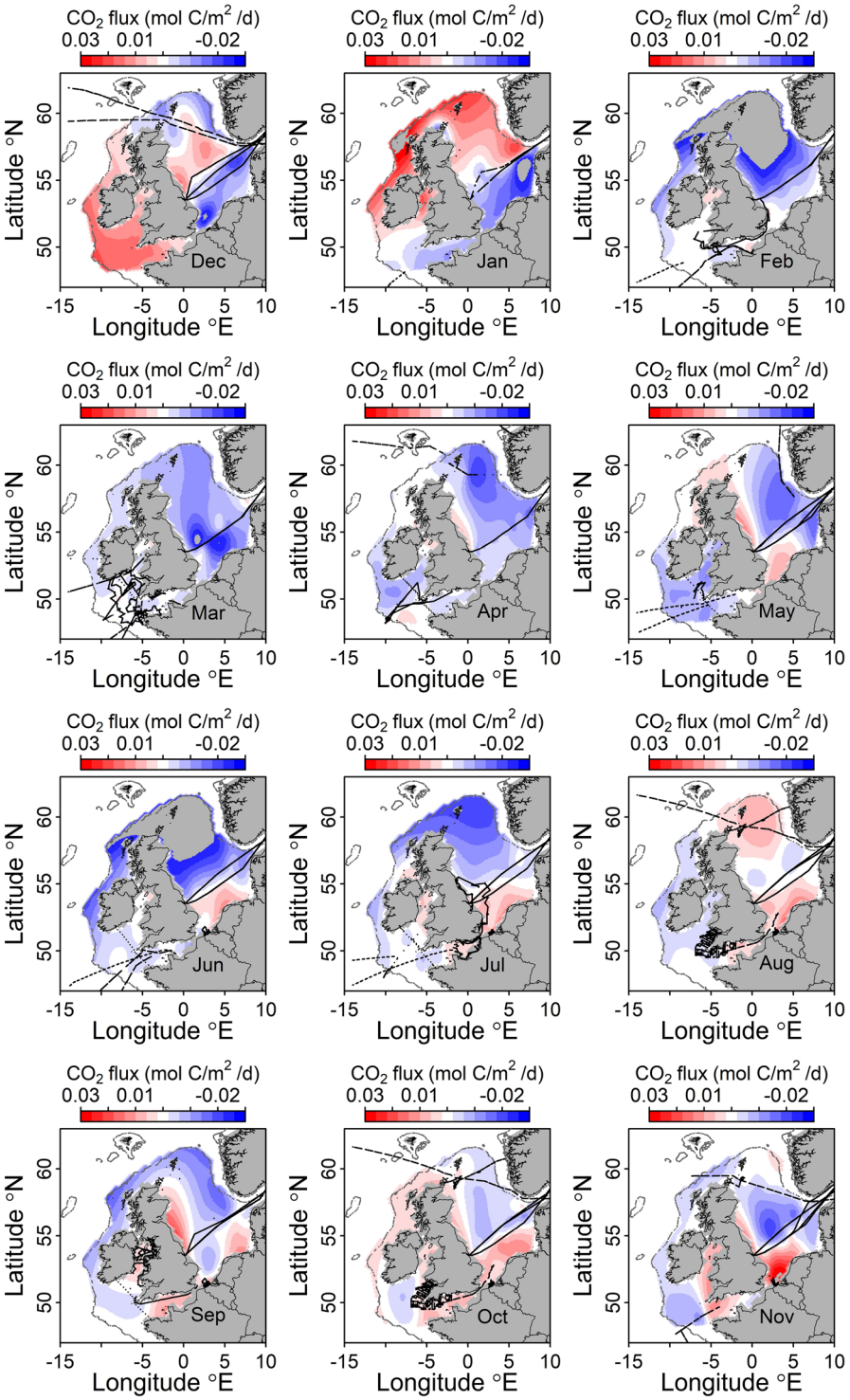

Figure 1. Monthly mean air-sea CO_2 flux for the NW European shelf in 2015 (negative values denote influx from the air). Note that December is grouped with January-February in the first row (winter). Black dotted lines indicate ship tracks.

biological + mixing flux-component rather than high thermal-flux component in these regions. A notable exception was the Irish Sea where the net biological + mixing component was negative.

C-budget terms. Table 1 lists the C-budget terms considered in our study (mean ± standard deviation of corresponding estimates listed in Table 1). The mean multi-year air to sea flux term was calculated as 23.0 ± 4.3 Tg C y^{-1}. Baltic Sea C-inputs contribute 12.6 ± 2.7 Tg C y^{-1} to the NW European shelf: 89% as DIC, the remainder as

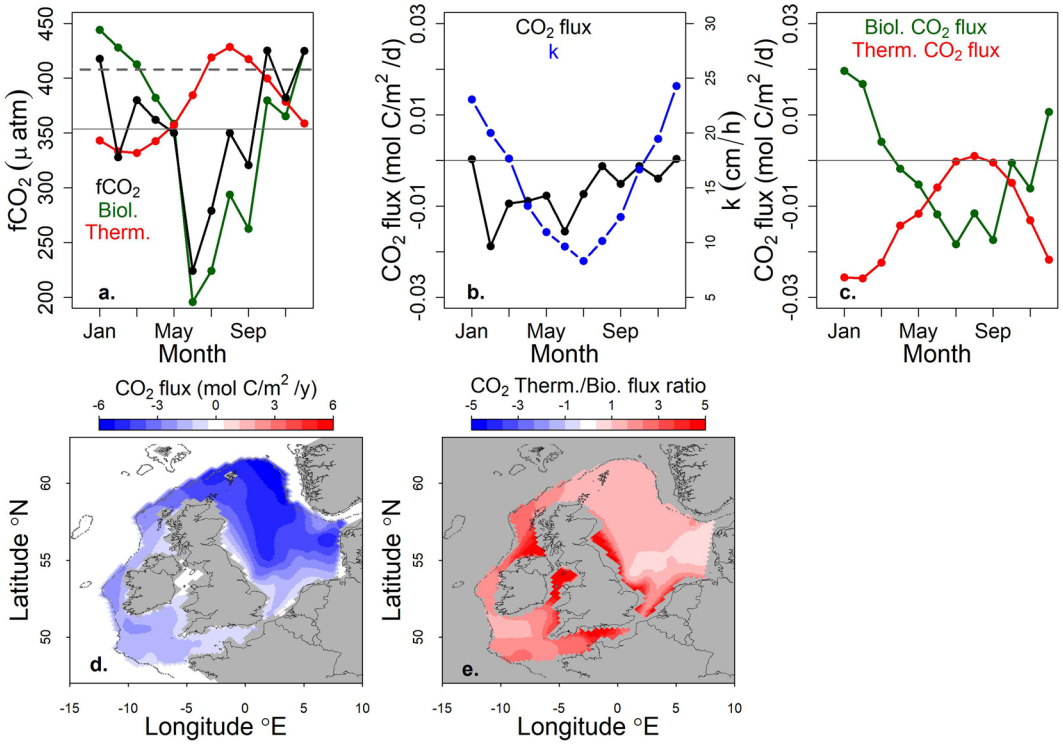

Figure 2. (**a**) Seasonal evolution of the mean $fCO_{2\,sea}$ (black) and its thermal (red) and biological + mixing (green) components (the solid and dashed horizontal lines represent mean seawater and atmospheric fCO_2 respectively), (**b**) seasonal evolution of the mean air to sea CO_2 flux (black) and the gas transfer velocity k (blue) (the horizontal line represents zero flux), (**c**) the thermal (red) and biological + mixing (green) components of the flux (the horizontal line represents zero flux), (**d**) annual air to sea CO_2 flux (negative values denote influx from the atmosphere), (**e**) annual ratio of the thermal to biological + mixing components of CO_2 flux (in our study, the ratio was only negative where the biological component was negative, i.e. the thermal component was always positive denoting influx).

organic-C. Rivers, were a smaller source of C contributing 2.4 ± 0.3 Tg C y^{-1} of DOC. The sum of pre-estuarine inputs was 21.6 Tg C y^{-1} while estuarine CO_2 efflux to the atmosphere was calculated as 24.4 ± 10.4 Tg C y^{-1}.

Our C-burial calculations showed that N_{ret} accounted for 63%, 91% and 97% of N_{dep} in mud, mud-sand and sand sediments respectively (each with an uncertainty of ±22%). Assuming that the conditions in March were representative of the low-productivity (i.e. net respirations) half of the year (winter) and the average of the May and August were representative of the high productivity half (spring and summer), we calculated annual net C-burial as 0.569 mol C m^{-2} y^{-1}, 0.055 mol C m^{-2} y^{-1} and 0.008 mol C m^{-2} y^{-1} for mud, mud-sand and sand respectively. The annual net C-burial over the NW European shelf was 1.3 ± 3.1 Tg C y^{-1}. This was therefore a small, but highly uncertain, loss term for shelf-sea C. The DIC accumulation rate, related to OA, was further scaled for the shelf area (1.06×10^{12} m^2) and mean depth (78.3 m) to yield 1.0 ± 0.5 Tg C y^{-1}. We acknowledge that this will vary regionally depending on the buffering capacity of seawater and other factors.

Finally, net exchange of C between the shelf and the open ocean via the CSP and advection was calculated as -34.4 ± 6.0 Tg C y^{-1} from the sum of the input terms (from the atmosphere, rivers and the Baltic Sea) minus C-burial and DIC accumulation. The uncertainty of our export-estimate is the standard error of the uncertainties in the other terms. Our estimate of the CSP is consistent with a previous estimate of 32.8 Tg C y^{-1} [26], which was based on the distribution of DIC in the North Sea. A further study estimated a monthly export of 2.2 Tg C via the Norwegian trench in late summer[27], which yields 27.2 Tg C y^{-1} if extrapolated over the whole year.

Discussion

Over the last two decades, a number of studies have quantified the air to sea flux of CO_2 over the NW European shelf, regions within it or the wider European shelf[25,28–30]. When scaled to their respective areas, these estimates (including our own) fall in the range of 1.3–2.1 mol C m^{-2} y^{-1} with a mean value of 1.8 ± 0.3 mol C m^{-2} y^{-1} (Table 1). This is three-fold higher than the average open ocean influx of 0.60 mol C m^{-2} y^{-1} [20], but lower than some high latitude seas (e.g. the Barents Sea: 4 mol C m^{-2} y^{-1} [31]) and upwelling systems (e.g. the South African coastal region: 3.83 mol C m^{-2} y^{-1} [32]). Our study provides the first such estimate based on observations collected in a single year. This offers unique advantages for understanding inter-annual variability related to climate and weather. For example, previous work has shown that the North Atlantic Oscillation (NAO; the dominant climate mode over the North Atlantic and a major influence on weather in NW Europe) exerts a strong influence on $fCO_{2\,sea}$ distribution in the North Sea[33]. In the absence of comparable, annual data this could not be explored

Flux type	Flux (Tg C y^{-1})	Reference
River	**$\Sigma(\overline{DOC})$ 2.4 ± 0.3**	
DOC	2.6	post-estuary; scaled from[24]
	2.1	pre-estuary; scaled from[26]
POC	0.6	pre-estuary; scaled from[24]
DIC	2.0	post-estuary; scaled from[24], accounted in air-sea flux
	18.9	pre-estuary; scaled from[26], accounted in estuarine- (24.4 ± 10.4 Tg C y^{-1}) and shelf- air to sea flux
Baltic Sea	**$\Sigma(\overline{DOC} + \overline{DIC})$ 12.6 ± 2.7**	
DOC	0.8	[71]
	1.9	[72]
	1.1	[26]
	1.9	[73]
DIC	9.7	[72]
	12.7	[26]
Air to Sea	23.0 ± 4.3	
	26.2	this study
	26.9	Scaled from[28]
	19.8	Scaled from[25],
	17.2	[29]
	25.0	Scaled from[26] – as recalculated by[30]
DIC accum.	−1.0 ± 0.5	
	−0.6	for ΔpH = −0.0013 units y^{-1} [69]
	−1.0	for ΔpH = −0.0022 units y^{-1} [42]
	−1.5	for ΔpH = −0.0035 units y^{-1} [43]
Sed. burial	−1.3 ± 3.1	
	−1.8	scaled from[26]
	−0.9 ± 2.5	this study
Export	−34.4 ± 6.0	this study – mass balance assuming that 50% of river-DOC is mineralized and accounted for in the air to sea flux

Table 1. C-fluxes into and out of (negative) the NW European Shelf (values in bold represent the mean ± standard deviation of the estimates listed below each flux). Some terms are listed here for information but accounted in other terms and therefore do not contribute to the mean flux (e.g. the river-DIC input is accounted in the estuarine and shelf air to sea flux and therefore not included in the river-flux). The terrestrial input only considers dissolved organic carbon (DOC), as dissolved inorganic carbon (DIC) is implicitly accounted for in the air to sea flux. The air to sea flux estimate by[25] was recalculated using 1.4 mol C m^{-2} y^{-1} for the North Sea, 0 mol C m^{-2} y^{-1} for the English Channel, and 1.0 mol C m^{-2} y^{-1} for the Celtic Sea, Faroes, North Scottish shelf, West Scottish shelf, West Irish shelf, Irish Sea and North Channel – and subsequently corrected for the wind reanalysis by Meyer *et al.* (2018). Note that the annual accumulation in DIC (DIC accum.) is negative here – otherwise it would count against export. Export via the CSP and advection was calculated as the difference between inputs and C-burial + OA, assuming that 50% of the river-DOC input is mineralized on the shelf (and therefore accounted for in the air to sea flux).

further (for reference, the 2015 winter-NAO index was positive, associated with above average precipitation and temperatures over our domain). We found that the 2015 influx of atmospheric CO_2 was dominated by the winter months (January to March and December) despite the small air-sea concentration gradient during this period. This conclusion is further supported by the flux component analysis (thermal vs. biological + mixing) which showed thermal influx dominance over a whole year. Nevertheless, we acknowledge that the flux component analysis creates an artificial situation whereby the expected thermal summer-efflux does not materialize because of net biological drawdown of $fCO_{2\,sea}$ at that time. Peak influx of CO_2 in winter, and/or due to high wind speeds and solubility, has also been observed in other shelf-seas[34].

The paucity of single-year studies leaves a number of open questions relating to the inter-annual persistence of the pattern observed in 2015 where the winter air to sea CO_2 flux was the dominant component of the net flux. Numerical models may be used to address this, but these are not entirely consistent with observations. Modelling studies for the NW European shelf are within ±50% of observation-based estimates [e.g. 1.5–2.6 mol C m^{-2} y^{-1} for the North Sea[7,35] compared to 1.8 ± 0.3 mol C m^{-2} y^{-1} for observations[25,28–30]]. Wider disagreement is found for long-term climate projections of wind speed (e.g. CMIP5) where different models predict increase or decrease in extreme wind events[36]. If wind speed is critical in determining the overall annual influx of CO_2 from the atmosphere (as shown here), it follows that model projections of this influx are equally contradictory and therefore uncertain.

Our synthesis of C-fluxes showed that the air to sea flux is the largest input term over the open NW European shelf (Fig. 3). River-borne C-inputs are largely lost in estuaries with CO_2 efflux accounting for the majority of

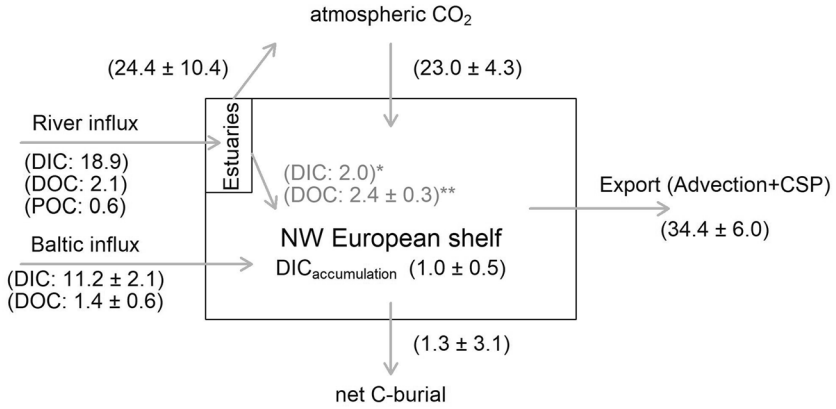

Figure 3. C-fluxes across the NW European shelf based on the present study and literature. Export is calculated as the difference between input/output terms and further subtracting the DIC accumulation term. (*): The post-estuarine DIC input is not considered in the calculation of export as it contributes to the air to sea flux and is therefore implicitly accounted for in this term. (**): We have arbitrarily assumed that 50% of post-estuarine river-DOC input is mineralized to CO_2 on the shelf – this is implicitly accounted for in the air to sea flux and does not contribute to export.

this loss. It should be noted that the estuarine CO_2 efflux to the atmosphere is biased towards larger estuaries where measurements exist – these are also more urbanized/industrialised and have longer residence times for degassing and mineralization to take place. In smaller estuaries with short residence times the river-borne C-load may bypass the estuarine filter and contribute to the air-sea flux over the open shelf. Any river-DIC input which passes the estuarine filter (and therefore contributes to exchange with the atmosphere) will modify the shelf DIC and by extension shelf-$fCO_{2\ sea}$. Since this was measured through our observation network, the post estuarine DIC-input was implicitly accounted for in the air to sea flux over the shelf and should not be considered further in order to avoid double-counting. Mineralization of river-DOC to CO_2 would likewise modify shelf-$fCO_{2\ sea}$ and be accounted for in the air to sea flux. The rapid decline of organic-C with distance offshore suggests that very little of this material contributes to export from the shelf[37,38]. The majority of organic-C from rivers must therefore be either buried or microbially/photochemically mineralized to CO_2[24,26]. However, a recent study in the North Sea showed conservative mixing between DOM optical characteristics with increasing salinity suggesting simple dilution between river- and oceanic-DOM[37]. Some river-DOC must therefore be exported past the shelf and into the open ocean as indicated by the presence of terrestrial DOM in the deep ocean[39]. For the synthesis presented in Fig. 3, we therefore arbitrarily assume that half of post-estuarine DOC input is mineralized on the shelf (and accounted for in the influx from the atmosphere) while the other half contributes to export. Conversely, the Baltic input is likely to contribute more to the export and advection term, both as DIC and DOC because of the shorter residence time of this input in the North Sea. Most of the C exported from the NW European shelf exits through the Norwegian trench following the clockwise circulation around the British Isles, eastward flow through the English Channel and counter-clockwise circulation in the North Sea[26]. Consequently, the residence time in the Norwegian Trench (i.e. in proximity to the Baltic inflow) is in the order to 100 days compared to months/years elsewhere in the North Sea[40]. This difference in residence times allows for the Baltic C-input to be exported from the shelf via the CSP and advection to the north, while river-inputs are subject to outgassing and/or mineralization on the shelf.

Our calculation of net C-burial is consistent with previous work showing that most of the organic-C produced annually in shelf-seas is recycled rather than buried in sediments[41]. A previous estimate for North Sea net C-burial was within the uncertainty of our estimate [0.9 Tg C y^{-1} for the North Sea, scaled here for the larger surface area of our study = 1.8 Tg C y^{-1} [26]]. Nevertheless, the C-burial term carries the largest proportional uncertainty. Although it is a relatively small term in this budget, net C-burial is of great interest as it provides a climate-regulation service by removing C from the contemporary C-cycle. The fate of C exported via the CSP and advection to the north is unclear, only providing a climate regulation service if it is entrained in intermediate and deep waters of the open ocean.

There is significant uncertainty in our estimate of the estuary to atmosphere CO_2 flux. Conservation of mass dictates that if this term changed then export via the CSP and advection should also change (other input/output terms were better constrained in our analysis). Considering lower and upper limits for the estuarine efflux of CO_2 to the atmosphere leads to the conclusion that the corresponding lower and upper limits for the export term would be 24 Tg C y^{-1} and 44.8 Tg C y^{-1} respectively. Independent estimates of the export term are consistent with our export estimate of 34.4 Tg C y^{-1}. Our conclusion that nearly all of the supply of DIC to estuaries is lost to the atmosphere within estuaries, is therefore plausible. However there is considerable work to do on refining our estimates of this term. In this respect, it is important to note that our budget only considered estuarine and shelf 'open water' and did not include salt-marshes and other 'blue carbon' stores, which are important sinks for C, but beyond the scope of this study. The suggestion that the riverine input of DIC and DOC to estuaries is largely lost to the atmosphere within those systems means that the open shelf net air to sea CO_2 flux is at present largely

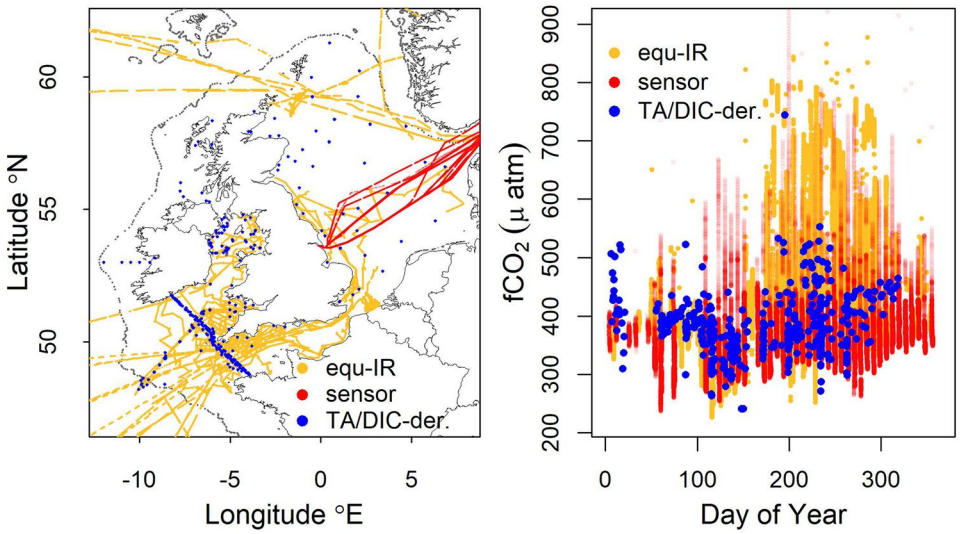

Figure 4. Spatial (left) and temporal (right) data coverage for fCO_2 observations by three methods.

decoupled from terrestrial influence. Land-management policies which might alter the delivery of organic-C to the NW European shelf (e.g. restoration of peat-bogs) would only have a modest effect on the open-shelf air to sea CO_2 flux, burial and export-terms since the river-DOC input is a relatively small term. Instead, the impact of varying river C-loads would likely be more pronounced in estuaries where some DOC-mineralization takes place and contributes to efflux of CO_2. Changes in river nutrient concentrations driven by environmental policy would be expected to affect net primary production and concomitant drawdown of atmospheric CO_2. However, if the majority of atmospheric CO_2 influx is shown to consistently take place during winter (as shown here for 2015) then the impact of such policies (designed to reduce eutrophication and improve the health of the coastal environment) on the open shelf sink of atmospheric CO_2 will be limited. As was the case for river-C loads, the impact of varying river nutrient loads is likely more pronounced in estuarine and near-shore environments.

Arguably the largest implications for the air to sea CO_2 flux relate to global CO_2 emission reduction policy. The most pertinent questions relate to the longevity of the shelf uptake of atmospheric CO_2 when the latter is continuously increasing. Long-term studies have shown that the accumulation of DIC is more rapid on the NW European shelf than elsewhere, leading to higher rates of OA in the range of -0.0022 to -0.0035 pH units y^{-1} [42,43], compared to $-0.0018 \pm 0.0004\,y^{-1}$ globally[44]. This may be evidence that export via the CSP and advection is becoming saturated in agreement with a modelling study which further predicted a negative feedback (decrease) on the air to sea flux[10]. Yet, comparing our 2015 air to sea CO_2 flux to previous estimates based on observations in the 1990s and 2000s does not support a reduction in atmospheric CO_2 influx. Continued international efforts under the global ocean acidification observing network (http://goa-on.org/), ICOS network[45] and others are essential to help us understand, identify and ultimately predict changes in the annual shelf-sea uptake of atmospheric-CO_2.

Methods

The NW European shelf is hereby defined as the region within the 200 m isobaths north of 47 °N and 8.5 °E. Based on a dataset of 298500 *in situ* observations of CO_2 fugacity (Supplementary Table 1) we calculated the air to sea flux of CO_2 using the open-source FluxEngine toolbox for 2015[46]. The dataset comprised three different method classes: a) continuous-flow equilibrator with partial drying of the headspace gas stream and infra-red detection following the recommendations of Pierrot *et al.*[47] (equ-IR; 99.9 k observations), b) fCO_2 derived from discrete measurements of Total Alkalinity and Dissolved Inorganic Carbon (TA/DIC-derived; 0.7 k observations) using the CO2SYS software package[48] and c) fCO_2 measured with a CONTROS HydroC CO_2 flow-through sensor[49] (sensor; 198 k observations) (Fig. 4). Further methodological details are given in the Supplementary Information.

Each method for the determination of fCO_2 carries a certain analytical uncertainty defined by its respective precision and accuracy, which, in turn, are influenced by properties such as instrument-drift, calibration frequency, equilibration timescale and resolution[50,51]. In order to quantify the internal consistency of observations we examined 'crossovers' between different datasets and for the three method classes (see Supplementary Information for details). A crossover was defined as a maximum distance of 40 km between observations, using 30 km as the equivalent distance for one day (e.g. two data-points, one day apart in time and 10 km apart in space, yield a nominal equivalent 'distance' between data-points of 40 km). The crossover analysis revealed a correlation between the three different method classes ($R^2 > 0.998$) with linear slopes (bias) statistically indistinguishable from unity. These statistics attest to the validity of the crossover analysis whilst the addition of 'salinity and temperature agreement' criteria (<0.2 and <0.5 °C respectively) further minimized the influence of river plumes and advection. There was therefore no systematic bias by any of the measurement techniques, which enabled us to use the whole dataset for calculating air-sea fluxes. We calculated a weighted uncertainty of 13.2 µatm for the whole dataset (note that this is not the accuracy which had a weighted mean value of 4 µatm based on the accuracy of individual systems; see Supplementary Information). Whilst we stress that this was not a strict inter-comparison

of methods, it nevertheless provides confidence in the dataset consistency as a whole and provides a useful metric to propagate in the calculation of flux uncertainty.

All instantaneous and integrated air-sea gas fluxes were calculated using the freely available FluxEngine toolbox[46]. The air-sea flux of CO_2 was calculated from the following equation:

$$F = k \times (\alpha_{sea} \times fCO_{2\,sea} - \alpha_{air} \times fCO_{2\,air}), \quad (1)$$

where k is the gas transfer velocity (units: cm h^{-1}), α_{sea} is the solubility of CO_2 at the bottom of the mass boundary layer and within the seawater (a function of salinity and temperature; units: g m^{-3} μatm^{-1}), α_{air} is the equivalent solubility at the top of the mass boundary layer (the air-side solubility; units: g m^{-3} μatm^{-1}), $fCO_{2\,sea}$ and $fCO_{2\,air}$ are the fugacity of CO_2 in seawater and air respectively (units: μatm).

$fCO_{2\,sea}$ data were re-analyzed to be valid for a consistent sea surface (sub-skin) temperature dataset and depth[52] using a climate quality (sub-skin) satellite temperature dataset[53]. These $fCO_{2\,sea}$ data (valid for the sub-skin and assumed to represent the bottom of the mass boundary layer) were then spatially interpolated (Data Interpolating Variation Analysis, DIVA v 4.7.1)[54] to a 50 km polar stereographic grid. A cool skin correction of −0.17 °C was used[55] to enable the calculation of skin temperature (using the sub-skin dataset as a reference) and thus the air-side solubility α_{air}. Atmospheric $fCO_{2\,air}$ was calculated within FluxEngine using the air pressure at the sea surface (European Centre for Medium Range Weather Forecasting re-analysis; https://www.ecmwf.int/en/research/climate-reanalysis/era-interim) and *in-situ* CO_2 dry air mole fraction from the National Oceanic and Atmospheric Administration Earth System Research Laboratory[56]. The atmospheric fCO_2 dataset used here offers a well characterized, quality controlled, 'clean' and consistent dataset for the calculation of flux. Wind speed (U_{10}) data were obtained from the Cross-Calibrated Multi-Platform (CCMP) version 2[57]. Salinity data came from the World Ocean Atlas 2013[58]. We used a quadratic wind driven parameterization of the gas transfer velocity[59] that was originally developed using shelf sea measurements. All input data were re-gridded to the 50 km polar stereographic grid. Total uncertainties in the air to sea flux calculations solely due to the input data were calculated using an ensemble method. Twenty five sets of calculations were made, with fCO_2, SST and U_{10} inputs perturbed by random noise representing the known uncertainties of the input parameters; $\sigma(fCO_2) = 13.2$ μatm; $\sigma(U_{10}) = 0.44$ ms^{-1}; σ(SST skin and sub-skin) = 0.6 °C. This ensemble gave an air-sea flux uncertainty of ±2%.

In order to investigate uncertainties arising from the DIVA interpolation of $fCO_{2\,sea}$, we compared the interpolated outputs with independent $fCO_{2\,sea}$ data from a buoy in the Western English Channel ($fCO_{2\,buoy}$ at station L4 operated by PML and not included in the combined fCO_2 dataset described above; see Supplementary Information for details). The corresponding daily air to sea flux (F_{buoy}) was computed using the same parameters as in FluxEngine (i.e. with the same *k*, α_{sea}, α_{air}, and $fCO_{2\,air}$), apart from the $fCO_{2\,sea}$ field. The daily flux using $fCO_{2\,buoy}$ was not significantly different from the corresponding monthly flux using the combined fCO_2 dataset described above (paired t-test; $t = -9.34$, $p < 0.001$, $n = 184$). Nevertheless, the 95% confidence interval 0.003 mol m^{-2} $month^{-1}$ represented an uncertainty of 16% of the annual flux at L4 when extrapolated for the whole year. The maximum total uncertainty from mapping and the ensemble runs described above (perturbations of fCO_2, U_{10} and SST) was therefore 18%. An additional 5% uncertainty arises from three quadratic parameterizations of *k* for the North Atlantic[60]. However, the ongoing debate regarding the optimum parameterization of *k* is beyond the scope of this paper and not considered further.

We separated the mean fCO_2 for each 50 km grid cell into its biological + mixing (Eq. 2) and thermal components (Eq. 3)[20].

$$fCO_{2\,bio} = fCO_{2\,sea} \times e^{(0.0423 \times (\overline{SST} - SST))}, \quad (2)$$

$$fCO_{2\,therm} = \overline{fCO_{2\,sea}} \times e^{(0.0423 \times (SST - \overline{SST}))}, \quad (3)$$

where fCO_2 and $\overline{fCO_2}$ are the observed and annual mean fCO_2 for each grid cell, SST and $\overline{SST}$ are the observed and annual mean sea surface temperature respectively (sub skin). $fCO_{2\,therm}$ and $fCO_{2\,bio}$ were subsequently used to replace $fCO_{2\,sea}$ in Eq. 1 in order to derive the respective flux components.

C-burial in shelf sediments was calculated for three sites in the Celtic Sea: a) a muddy sediment (51.2114 °N, 6.1338 °W), b) a sandy sediment (51.0745 °N, 6.5837 °W) and c) a mud-sand sediment (station CCS: 49.4117 °N, 8.5985 °W). The following biogeochemical rates were determined at these sites in March (end of winter), May (during the spring bloom) and August 2015 (late summer): benthic oxygen consumption (Resp = respiration), nitrification (Nit), denitrification (Den), anammox (Ax) and sediment-water inorganic-N fluxes (FN; for $NO_3^- + NO_2^- + NH_4^+$) (e.g. Supplementary Table 3)[61]. Our general reasoning for the C-burial calculation relies on the conservation of mass and specified C:N ratios in organic matter, where near-closure of the C-cycle is assumed *a priori* and tested against closure of the N-cycle *a posteriori* (see Supplementary Information for calculations).

In order to provide context for the air to sea flux we further considered C-inputs to the NW European shelf from rivers and the Baltic inflow as well as loss-terms from the shelf (estuarine degassing, C-burial in sediments and export via the CSP and advection). For this purpose, we constructed a balanced budget where the CSP+ advection term were the remainder of all other terms.

Firstly, we combined our 2015 estimate of air to sea CO_2 flux with previous studies to obtain a mean influx term from the atmosphere[25,28–30].

River-borne C enters the NW European shelf in a buoyant, low-salinity layer and must first transit through estuaries where CO_2-outgassing as well as organic-C burial and/or mineralization moderate the river-borne C-input to the shelf[62–65]. We therefore used a previous estimate of C-export from European rivers north of 50 °N (5.4×10^{-6} Tg C y^{-1} km^{-2}; after the estuarine filter)[24], scaled to the catchment area of rivers in our domain

[892×10^3 km^2 [66]] to estimate a post-estuarine input of 4.8 Tg C y^{-1}. This was further separated into DIC (41.1%), DOC (54.3%) and POC (4.4%)[24]. The latter (0.2 Tg C y^{-1}) is thought to be trapped in estuaries where it contributes to C-burial and outgassing[24] and is therefore not considered further as an input to the NW European shelf. By comparison, the freshwater-endmember (i.e. pre-estuarine) of C-inputs to the North Sea[26], scaled to the shelf area in our domain, yielded 18.9 Tg C y^{-1} and 2.1 Tg C y^{-1} for DIC and DOC respectively. The estimates of Ciais *et al.* (2008) and Thomas *et al.* (2005) are roughly in agreement for DOC, but differ by one order of magnitude for DIC. However, correcting the higher estimate of Thomas *et al.* (2005) for CO_2 outgassing could easily account for this difference. We estimate the estuarine efflux of CO_2 to the atmosphere as 24.4 ± 10.4 Tg C y^{-1}, based on: a) estuarine sea to air efflux of 19.8–62.0 mol C m^{-2} y^{-1}[25,62,65,67]; b) the ratio of estuarine area to coastline length of 2.64 km^2 km^{-1} [68]; and c) the coastline length of the domain considered here (18204 km).

As a result of long-term, net CO_2 influx from the atmosphere and lateral advection from the open ocean, the NW European shelf is gaining C in the form of DIC which causes Ocean Acidification (OA). Whilst this is not an input term, it does not contribute to export via the CSP+ advection and must therefore be accounted for as the latter is the remainder of input vs output terms. In our study, this DIC accumulation rate was estimated from annual OA rates in the range of - 0.0013 to −0.0035 pH-units[42,43,69]. We estimated a mean DIC accumulation rate of 1.01 µmol kg^{-1} y^{-1} using the CO2SYS software[48] with $pH_T = 8.05$ and Total Alkalinity of 2283.1 µmol kg^{-1} [70] as baseline.

Data availibility

All fCO_2 data used in this study are available from the SOCAT and Ferrybox databases (www.socat.info and www.ferrybox.org).

Received: 4 June 2019; Accepted: 6 December 2019;
Published online: 27 December 2019

References

1. Cai, W. J., Dai, M. H. & Wang, Y. C. Air-sea exchange of carbon dioxide in ocean margins: A province-based synthesis. *Geophysical Research Letters* **33**, L12603, https://doi.org/10.1029/2006gl026219 (2006).
2. Chen, C. T. A. & Borges, A. V. Reconciling opposing views on carbon cycling in the coastal ocean: Continental shelves as sinks and near-shore ecosystems as sources of atmospheric CO_2. *Deep-Sea Res. Part II-Top. Stud. Oceanogr.* **56**, 578–590, https://doi.org/10.1016/j.dsr2.2009.01.001 (2009).
3. Laruelle, G. G., Durr, H. H., Slomp, C. P. & Borges, A. V. Evaluation of sinks and sources of CO(2) in the global coastal ocean using a spatially-explicit typology of estuaries and continental shelves. *Geophysical Research Letters* **37**, https://doi.org/10.1029/2010gl043691 (2010).
4. Caldeira, K. & Wickett, M. E. Anthropogenic carbon and ocean pH. *Nature* **425**, 365–365 (2003).
5. Weiss, R. F. Carbon dioxide in water and seawater: the solubility of a non-ideal gas. *Marine Chemistry* **2**, 203–215 (1974).
6. Laruelle, G. G. *et al.* Continental shelves as a variable but increasing global sink for atmospheric carbon dioxide. *Nature Communications* **9**, https://doi.org/10.1038/s41467-017-02738-z (2018).
7. Gröger, M., Maier-Reimer, E., Mikolajewicz, U., Moll, A. & Sein, D. NW European shelf under climate warming: implications for open ocean - shelf exchange, primary production, and carbon absorption. *Biogeosciences* **10**, 3767–3792, https://doi.org/10.5194/bg-10-3767-2013 (2013).
8. Holt, J., Butenschon, M., Wakelin, S. L., Artioli, Y. & Allen, J. I. Oceanic controls on the primary production of the northwest European continental shelf: model experiments under recent past conditions and a potential future scenario. *Biogeosciences* **9**, 97–117, https://doi.org/10.5194/bg-9-97-2012 (2012).
9. Tsunogai, S., Watanabe, S. & Sato, T. Is there a "continental shelf pump" for the absorption of atmospheric CO_2? *Tellus Series B-Chemical and Physical Meteorology* **51**, 701–712, https://doi.org/10.1034/j.1600-0889.1999.t01-2-00010.x (1999).
10. Bourgeois, T. *et al.* Coastal-ocean uptake of anthropogenic carbon. *Biogeosciences* **13**, 4167–4185, https://doi.org/10.5194/bg-13-4167-2016 (2016).
11. Forzieri, G. *et al.* Ensemble projections of future streamflow droughts in Europe. *Hydrol. Earth Syst. Sci.* **18**, 85–108, https://doi.org/10.5194/hess-18-85-2014 (2014).
12. Stahl, K., Tallaksen, L. M., Hannaford, J. & van Lanen, H. A. J. Filling the white space on maps of European runoff trends: estimates from a multi-model ensemble. *Hydrol. Earth Syst. Sci.* **16**, 2035–2047, https://doi.org/10.5194/hess-16-2035-2012 (2012).
13. Council of the European Union. Council Directive 91/676/EEC of 12 December 1991 concerning the protection of waters against pollution caused by nitrates from agricultural sources. *Official Journal of the European Communities* **34**, 1–9 (1991).
14. Council of the European Union. Council Directive 91/271/EEC of 21 May 1991 concerning urban waste-water treatment. *Official Journal of the European Communities* **34**, 40–53 (1991).
15. Council of the European Union. Directive 2000/60/EC of the European Parliament and of the Council of 23 October 2000 establishing a framework for Community action in the field of water policy. *Official Journal of the European Communities* **43**, 1–73 (2000).
16. Council of the European Union. Directive 2008/56/EC of the European Parliament and of the Council of 17 June 2008 establishing a framework for community action in the field of marine environmental policy (Marine Strategy Framework Directive). *Official Journal of the European Communities* **51**, 19–40 (2008).
17. Monteith, D. T. *et al.* Dissolved organic carbon trends resulting from changes in atmospheric deposition chemistry. *Nature* **450**, 537–U539, https://doi.org/10.1038/nature06316 (2007).
18. Worrall, F., Howden, N. J. K., Burt, T. P. & Bartlett, R. Declines in the dissolved organic carbon (DOC) concentration and flux from the UK. *Journal of Hydrology* **556**, 775–789, https://doi.org/10.1016/j.jhydrol.2017.12.001 (2018).
19. Jackson, T., Sathyendranath, S. & Mélin, F. An improved optical classification scheme for the Ocean Colour Essential Climate Variable and its applications. *Remote Sensing of Environment* **(available online)**, https://doi.org/10.1016/j.rse.2017.1003.1036 (2016).
20. Takahashi, T. *et al.* Global sea-air CO_2 flux based on climatological surface ocean pCO(2), and seasonal biological and temperature effects. *Deep-Sea Res. Part II-Top. Stud. Oceanogr.* **49**, 1601–1622 (2002).
21. Williams, C., Sharples, J., Mahaffey, C. & Rippeth, T. Wind-driven nutrient pulses to the subsurface chlorophyll maximum in seasonally stratified shelf seas. *Geophysical Research Letters* **40**, 5467–5472, https://doi.org/10.1002/2013gl058171 (2013).
22. Broecker, W. S. & Peng, T. H. Gas-Exchange Rates between Air and Sea. *Tellus* **26**, 21–35 (1974).
23. Morel, A. & Prieur, L. Analysis of variations in ocean color. *Limnology and Oceanography* **22**, 709–722, https://doi.org/10.4319/lo.1977.22.4.0709 (1977).

24. Ciais, P. *et al*. The impact of lateral carbon fluxes on the European carbon balance. *Biogeosciences* **5**, 1259–1271, https://doi.org/10.5194/bg-5-1259-2008 (2008).
25. Borges, A. V., Schiettecatte, L. S., Abril, G., Delille, B. & Gazeau, E. Carbon dioxide in European coastal waters. *Estuar. Coast. Shelf Sci.* **70**, 375–387, https://doi.org/10.1016/j.ecss.2006.05.046 (2006).
26. Thomas, H. *et al*. The carbon budget of the North Sea. *Biogeosciences* **2**, 87–96 (2005).
27. Bozec, Y., Thomas, H., Elkalay, K. & de Baar, H. J. W. The continental shelf pump for CO_2 in the North Sea - evidence from summer observation. *Marine Chemistry* **93**, 131–147, https://doi.org/10.1016/j.marchem.2004.07.006 (2005).
28. Frankignoulle, M. & Borges, A. V. European continental shelf as a sink for atmospheric carbon dioxide. *Glob. Biogeochem. Cycle* **15**, 569–576 (2001).
29. Laruelle, G. G., Lauerwald, R., Pfeil, B. & Regnier, P. Regionalized global budget of the CO_2 exchange at the air-water interface in continental shelf seas. *Glob. Biogeochem. Cycle* **28**, 1199–1214, https://doi.org/10.1002/2014gb004832 (2014).
30. Meyer, M., Patsch, J., Geyer, B. & Thomas, H. Revisiting the Estimate of the North Sea Air-Sea Flux of CO_2 in 2001/2002: The Dominant Role of Different Wind Data Products. *Journal of Geophysical Research-Biogeosciences* **123**, 1511–1525, https://doi.org/10.1029/2017jg004281 (2018).
31. Lauvset, S. K. *et al*. Annual and seasonal fCO(2) and air-sea CO_2 fluxes in the Barents Sea. *J. Mar. Syst.* **113**, 62–74, https://doi.org/10.1016/j.jmarsys.2012.12.011 (2013).
32. Arnone, V., Gonzalez-Davila, M. & Santana-Casiano, J. M. CO_2 fluxes in the South African coastal region. *Marine Chemistry* **195**, 41–49, https://doi.org/10.1016/j.marchem.2017.07.008 (2017).
33. Salt, L. A. *et al*. Variability of North Sea pH and CO_2 in response to North Atlantic Oscillation forcing. *Journal of Geophysical Research-Biogeosciences* **118**, 1584–1592, https://doi.org/10.1002/2013jg002306 (2013).
34. Ingrosso, G. *et al*. Drivers of the carbonate system seasonal variations in a Mediterranean gulf. *Estuar. Coast. Shelf Sci.* **168**, 58–70, https://doi.org/10.1016/j.ecss.2015.11.001 (2016).
35. Wakelin, S. L. *et al*. Modeling the carbon fluxes of the northwest European continental shelf: Validation and budgets. *J. Geophys. Res.-Oceans* **117**, https://doi.org/10.1029/2011jc007402 (2012).
36. de Winter, R. C., Sterl, A. & Ruessink, B. G. Wind extremes in the North Sea Basin under climate change: An ensemble study of 12 CMIP5 GCMs. *Journal of Geophysical Research: Atmospheres* **118**, 1601–1612, https://doi.org/10.1002/jgrd.50147 (2013).
37. Painter, S. C. *et al*. Terrestrial dissolved organic matter distribution in the North Sea. *Science of the Total Environment* **630**, 630–647, https://doi.org/10.1016/j.scitotenv.2018.02.237 (2018).
38. Massicotte, P., Asmala, E., Stedmon, C. & Markager, S. Global distribution of dissolved organic matter along the aquatic continuum: Across rivers, lakes and oceans. *Science of the Total Environment* **609**, 180–191, https://doi.org/10.1016/j.scitotenv.2017.07.076 (2017).
39. Medeiros, P. M. *et al*. A novel molecular approach for tracing terrigenous dissolved organic matter into the deep ocean. *Glob. Biogeochem. Cycle* **30**, 689–699, https://doi.org/10.1002/2015GB005320 (2016).
40. Blaas, M., Kerkhoven, D. & de Swart, H. E. Large-scale circulation and flushing characteristics of the North Sea under various climate forcings. *Climate Research* **18**, 47–54, https://doi.org/10.3354/cr018047 (2001).
41. de Haas, H., van Weering, T. C. E. & de Stieger, H. Organic carbon in shelf seas: sinks or sources, processes and products. *Continental Shelf Research* **22**, 691–717, https://doi.org/10.1016/s0278-4343(01)00093-0 (2002).
42. Clargo, N. M., Salt, L. A., Thomas, H. & de Saar, H. J. W. Rapid increase of observed DIC and pCO(2) in the surface waters of the North Sea in the 2001-2011 decade ascribed to climate change superimposed by biological processes. *Marine Chemistry* **177**, 566–581, https://doi.org/10.1016/j.marchem.2015.08.010 (2015).
43. Ostle, C. *et al*. Carbon dioxide and ocean acidification observations in UK waters: Synthesis report with a focus on 2010–2015 (2016).
44. Lauvset, S. K., Gruber, N., Landschuetzer, P., Olsen, A. & Tjiputra, J. Trends and drivers in global surface ocean pH over the past 3 decades. *Biogeosciences* **12**, 1285–1298, https://doi.org/10.5194/bg-12-1285-2015 (2015).
45. Steinhoff, T. *et al*. Constraining the Oceanic Uptake and Fluxes of Greenhouse Gases by Building an Ocean Network of Certified Stations: The Ocean Component of the Integrated Carbon Observation System, ICOS-Oceans. *Frontiers in Marine Science* **6**, https://doi.org/10.3389/fmars.2019.00544 (2019).
46. Shutler, J. D. *et al*. FluxEngine: A Flexible Processing System for Calculating Atmosphere Ocean Carbon Dioxide Gas Fluxes and Climatologies. *Journal of Atmospheric and Oceanic Technology* **33**, 741–756, https://doi.org/10.1175/jtech-d-14-00204.1 (2016).
47. Pierrot, D. *et al*. Recommendations for autonomous underway pCO(2) measuring systems and data-reduction routines. *Deep-Sea Res. Part II-Top. Stud. Oceanogr.* **56**, 512–522, https://doi.org/10.1016/j.dsr2.2008.12.005 (2009).
48. Lewis, E. & Wallace, D. W. R. Program Developed for CO_2 System Calculations., ORNL/CDIAC-105. (Carbon Dioxide Information Analysis Center, Oak Ridge National Laboratory, U.S. Department of Energy, Oak Ridge, Tennessee., 1998).
49. Petersen, W. FerryBox systems: State-of-the-art in Europe and future development. *J. Mar. Syst.* **140**, 4–12, https://doi.org/10.1016/j.jmarsys.2014.07.003 (2014).
50. Dickson, A. G., Sabine, C. L. & Christion, J. R. Guide to best practices for ocean CO_2 measurements. *PICES Special Publication* **3**, 191 (2007).
51. Wanninkhof, R. *et al*. Incorporation of alternative sensors in the SOCAT database and adjustments to dataset Quality Control flags. (Carbon Dioxide Information Analysis Center, Oak Ridge National Laboratory, US Department of Energy Oak Ridge, Tennessee, http://cdiac.ornl.gov/oceans/Recommendationnewsensors.pdf, https://doi.org/10.3334/CDIAC/OTG.SOCAT_ADQCF, 2013).
52. Goddijn-Murphy, L. M., Woolf, D. K., Land, P. E., Shutler, J. D. & Donlon, C. The OceanFlux Greenhouse Gases methodology for deriving a sea surface climatology of CO_2 fugacity in support of air-sea gas flux studies. *Ocean Science* **11**, 519–541, https://doi.org/10.5194/os-11-519-2015 (2015).
53. Banzon, V., Smith, T. M., Chin, T. M., Liu, C. Y. & Hankins, W. A long-term record of blended satellite and *in situ* sea-surface temperature for climate monitoring, modeling and environmental studies. *Earth System Science Data* **8**, 165–176, https://doi.org/10.5194/essd-8-165-2016 (2016).
54. Troupin, C. *et al*. Generation of analysis and consistent error fields using the Data Interpolating Variational Analysis (DIVA). *Ocean Modelling* **52-53**, 90–101, https://doi.org/10.1016/j.ocemod.2012.05.002 (2012).
55. Donlon, C. J. *et al*. Implications of the oceanic thermal skin temperature deviation at high wind speed. *Geophysical Research Letters* **26**, 2505–2508, https://doi.org/10.1029/1999gl900547 (1999).
56. Dlugokencky, E. J. (ed NOAA ESRL Carbon Cycle Cooperative Global Air Sampling Network) (NOAA, Bremerhaven, 2016).
57. Atlas, R. *et al*. A cross-calibrated multiplatform ocean surface wind velocity product for meteorological and oceanographic applications. *Bulletin of the American Meteorological Society* **92**, 157–174, https://doi.org/10.1175/2010bams2946.1 (2011).
58. Zweng, M. M. *et al*. World Ocean Atlas 2013, Volume 2: Salinity. 39 (2013).
59. Nightingale, P. D. *et al*. *In situ* evaluation of air-sea gas exchange parameterizations using novel conservative and volatile tracers. *Glob. Biogeochem. Cycle* **14**, 373–387 (2000).
60. Wrobel, I. & Piskozub, J. Effect of gas-transfer velocity parameterization choice on air–sea CO_2 fluxes in the North Atlantic Ocean and the European Arctic. *Ocean Sci.* **12**, 1091–1103, https://doi.org/10.5194/os-12-1091-2016 (2016).
61. Kitidis, V. *et al*. Seasonal benthic nitrogen cycling in a temperate shelf sea: the Celtic Sea. *Biogeochemistry* **135**, 103–119, https://doi.org/10.1007/s10533-017-0311-3 (2017).
62. Frankignoulle, M. *et al*. Carbon dioxide emission from European estuaries. *Science* **282**, 434–436 (1998).

63. Borges, A. V. & Frankignoulle, M. Distribution of surface carbon dioxide and air-sea exchange in the English Channel and adjacent areas. *J. Geophys. Res.-Oceans* **108**, https://doi.org/10.1029/2000jc000571 (2003).
64. Borges, A. V., Delille, B. & Frankignoulle, M. Budgeting sinks and sources of CO_2 in the coastal ocean: Diversity of ecosystems counts. *Geophysical Research Letters* **32**, L14601, https://doi.org/10.1029/2005gl023053 (2005).
65. Chen, C. T. A. *et al*. Air-sea exchanges of CO_2 in the world's coastal seas. *Biogeosciences* **10**, 6509–6544, https://doi.org/10.5194/bg-10-6509-2013 (2013).
66. Billen, G. *et al*. In *The European Nitrogen Assessment* (eds M.A. Sutton *et al*.) Ch. 13, 271–297 (Cambridge University Press, 2011).
67. Cai, W. J. In *Annual Review* of Ma*rine Science, Vol 3* Vol. 3 *Annual Review of Marine Science* (eds C. A. Carlson & S. J. Giovannoni) 123–145 (2011).
68. Woodwell, G. M. & Pecan, E. V. *Carbon and the Biosphere*. (Technical Information Center, U.S. Atomic Energy Commission, 1973).
69. Kitidis, V., Brown, I., Hardman-Mountford, N. & Lefevre, N. Surface ocean carbon dioxide during the Atlantic Meridional Transect (1995–2013); evidence of ocean acidification. *Progress in Oceanography* **158**, 65–75, https://doi.org/10.1016/j.pocean.2016.08.005 (2017).
70. Salt, L. A., Thomas, H., Bozec, Y., Borges, A. V. & de Baar, H. J. W. The internal consistency of the North Sea carbonate system. *J. Mar. Syst.* **157**, 52–64, https://doi.org/10.1016/j.jmarsys.2015.11.008 (2016).
71. Osburn, C. L. & Stedmon, C. A. Linking the chemical and optical properties of dissolved organic matter in the Baltic-North Sea transition zone to differentiate three allochthonous inputs. *Marine Chemistry* **126**, 281–294, https://doi.org/10.1016/j.marchem.2011.06.007 (2011).
72. Kulinski, K. & Pempkowiak, J. The carbon budget of the Baltic Sea. *Biogeosciences* **8**, 3219–3230, https://doi.org/10.5194/bg-8-3219-2011 (2011).
73. Seidel, M. *et al*. Composition and Transformation of Dissolved Organic Matter in the Baltic Sea. *Front. Earth Sci*. **5**, https://doi.org/10.3389/feart.2017.00031 (2017).

Acknowledgements

This study was supported by the UK NERC and DEFRA funded Shelf Sea Biogeochemistry strategic research programme (NE/K00204X/1; NE/K00185X/1; NE/K001701/1; NE/K002058/1; NE/K001957/1; NE/K002007/1), ICOS-UK and UK NERC funding (CLASS Theme1.2, NE/R015953/1), German Federal Ministry of Education and Research (01LK1224I; ICOS-D), the Flemish contribution to the ICOS-project, the Norwegian Research Council (ICOS-Norway, 245927), the European Commission (CARBOCHANGE; grant agreement 264879), European Commission (JERICO-NEXT; Grant agreement 654410), the Institut de Recherche pour le Développement (IRD) and ICOS France. We would like to thank the officers and crew of the research and commercial ships which have been used for data collection. We thank the NERC Earth Observation Data Acquisition and Analysis Service (NEODAAS) for supplying Chlorophyll-a data for this study. $fCO_{2\,sea}$ data used in this study are available from the SOCAT and Ferrybox databases (www.socat.info and www.ferrybox.org).

Author contributions

V.K. designed the study and led the writing. J.D.S., I.A., M.W., P.E.L., D.D., B.G., A.C. contributed to Flux Engine work, I.B., H.F., S.H.E., M.H., C.K., N.G., T.H., D.P., T.Mc.G., B.M.S., P.W., E.Mc.G., Y.B., J.-P.G., Sv.H., M.H., U.S., T.J., A.O., S.K.L., I.S., A.O., T.S., A.K., M.B., N.L., T.G., A.C., W.P., Y.V. contributed fCO_2 data. All authors contributed to writing this manuscript.

Competing interests

The authors declare no competing interests.

Additional information

Supplementary information is available for this paper at https://doi.org/10.1038/s41598-019-56363-5.

Correspondence and requests for materials should be addressed to V.K.

Reprints and permissions information is available at www.nature.com/reprints.

Publisher's note Springer Nature remains neutral with regard to jurisdictional claims in published maps and institutional affiliations.